J. Cell. Mol. Med. Vol 13, No 9B, 2009 pp. 3497-3516

Control of chondrocyte gene expression by actin dynamics: a novel role of cholesterol/Ror-α signalling in endochondral bone growth

Anita Woods, Claudine G. James, Guoyan Wang, Holly Dupuis, Frank Beier *

CIHR Group in Skeletal Development and Remodeling, Department of Physiology and Pharmacology, Schulich School of Medicine and Dentistry, The University of Western Ontario, London, Ontario, Canada

Received: September 14, 2008; Accepted: January 14, 2009

Abstract

Elucidating the signalling pathways that regulate chondrocyte differentiation, such as the actin cytoskeleton and Rho GTPases, during development is essential for understanding of pathological conditions of cartilage, such as chondrodysplasias and osteoarthritis. Manipulation of actin dynamics in tibia organ cultures isolated from E15.5 mice results in pronounced enhancement of endochondral bone growth and specific changes in growth plate architecture. Global changes in gene expression were examined of primary chondrocytes isolated from embryonic tibia, treated with the compounds cytochalasin D, jasplakinolide (actin modifiers) and the ROCK inhibitor Y27632. Cytochalasin D elicited the most pronounced response and induced many features of hypertrophic chondrocyte differentiation. Bioinformatics analyses of microarray data and expression validation by real-time PCR and immunohistochemistry resulted in the identification of the nuclear receptor retinoid related orphan receptor-α (Ror-α) as a novel putative regulator of chondrocyte hypertrophy. Expression of Ror-α target genes, (*Lpl*, fatty acid binding protein 4 [*Fabp4*], *Cd36* and kruppel-like factor 5 [*Klf15*]) were induced during chondrocyte hypertrophy and by cytochalasin D and are cholesterol dependent. Stimulation of Ror-α by cholesterol results in increased bone growth and enlarged, rounded cells, a phenotype similar to chondrocyte hypertrophy and to the changes induced by cytochalasin D, while inhibition of cholesterol synthesis by lovastatin inhibits cytochalasin D induced bone growth. Additionally, we show that in a mouse model of cartilage specific (Col2-Cre) Rac1, inactivation results in increased Hif-1α (a regulator of *Rora* gene expression) and Ror-α^{+} cells within hypertrophic growth plates. We provide evidence that cholesterol signalling through increased Ror-α expression stimulates chondrocyte hypertrophy and partially mediates responses of cartilage to actin dynamics.

Keywords: chondrocytes • rho GTPases • actin cytoskeleton • microarray • cholesterol • nuclear receptors • Ror-α • hypertrophy

Introduction

The majority of the vertebrate appendicular and axial skeleton is formed by endochondral ossification, a developmental process that requires the formation of a cartilage template intermediate. Longitudinal growth of long bones is achieved through the activity of the growth plate, the cartilaginous structure that remains at either end of the bone [1]. The growth plate is a highly sophisticated tissue that is organized into three distinctive zones; resting, proliferative and hypertrophic. Each portion exhibits distinct cell morphology, organization and specific gene expression patterns [2]. Chondrocytes of the resting zone are small and surrounded by vast quantities of matrix [3]. The rate of proliferation of resting chondrocytes is slow in comparison to the proliferative zone [4]. Chondrocytes within the proliferative zone are distinguished by their columnar organization and discoidal shape [5]. The rate of proliferation is highest in this portion of the growth plate and chondrocytes expresses high levels of proliferative markers such as cyclin D1 [6]. Hypertrophic chondrocytes are cuboidal and much larger in volume, and this increase in size contributes greatly to longitudinal bone growth [7]. Hypertrophic chondrocytes also express a different subset of genes, such as type X

*Correspondence to: Frank BEIER,
Department of Physiology and Pharmacology,
University of Western Ontario, London, Ontario N6A 5C1, Canada.
Tel.: (519) 661–2111-85344
Fax: (519) 661–3827
E-mail: fbeier@uwo.ca

doi:10.1111/j.1582-4934.2009.00684.x

collagen, matrix metalloproteases (MMPs) and vascular endothelial growth factor-α (Vegf-α) [8]. Although many markers of chondrocyte differentiation are known, the signalling pathways regulating their expression remain incompletely understood.

Chondrodysplasias are a large family of diseases that are characterized by disordered cartilage development and bone formation resulting in dwarfism and poor bone quality [9, 10]. The pathways regulating chondrocyte hypertrophy are also implicated in osteoarthritis (OA). Ectopic chondrocyte hypertrophy has been demonstrated in OA, suggesting that the pathogenetical process involves a recapitulation of endochondral ossification [11–13]. Therefore, analyses of the molecular pathways regulating hypertrophy in development are of particular interest for understanding OA.

We recently identified a role of the actin cytoskeleton and the Rho family of small GTPases as major regulators of chondrocyte differentiation. Our data demonstrated that RhoA/ROCK signalling inhibits both early and late chondrocyte differentiation *in vitro* [14–16]. It has been previously shown that inhibiting actin polymerization re-establishes chondrocyte gene expression in de-differentiated chondrocytes *in vitro* [17–21]. We have also shown that manipulation of the actin cytoskeleton promotes the differentiation of mesenchymal cells to the chondrocyte lineage *in vitro* [14]. However, the effects of manipulating the actin cytoskeleton on later stages of chondrocyte differentiation are still unknown, as are most of the target genes mediating the chondrocyte response to changes in actin dynamics.

In this study, we have employed microarray analysis in order to understand global changes in chondrocyte gene expression in response to modifiers of the actin cytoskeleton. Additionally, we compare the current data set with previous gene expression data during chondrocyte differentiation *in vitro* and *in vivo*. Our data suggest that inhibition of actin polymerization promotes chondrocyte hypertrophy. We functionally analysed the retinoid related orphan receptor-α (Ror-α), a gene that was up-regulated in all three analysed models of chondrocyte maturation. Interestingly, several genes up-regulated by cytochalasin D treatment were also identified as known targets of Ror-α signalling. This suggests a novel pathway downstream of actin dynamics that controls chondrocyte hypertrophy through cholesterol/Ror-α signalling.

Materials and methods

Materials

CD1 mice (timed pregnant at embryonic day (E) 15.5) were purchased from Charles River Laboratories (St. Constant, Quebec, Canada). All cell culture reagents were from Invitrogen (Burlington, Ontario, Canada) unless stated otherwise. Y27632 (cat. #688000) and jasplakinolide (cat. #420107) were purchased from Calbiochem (Darmstadt, Germany), and cytochalasin D from Sigma Aldrich (St. Louis, MO, USA), cat. #C8273. General chemicals were from Sigma Aldrich or Calbiochem unless otherwise stated. The Ror-α antibody was purchased from Santa Cruz (Santa Cruz, CA, USA), cat. #sc-28612, the hypoxic inducible factor 1, subunit α (Hif-1α) antibody was purchased from Cell Signaling (Danvers, MA, USA), cat. #3716, and the β-actin antibody was from Sigma Aldrich (cat. #A3853).

Methods

Organ culture

Tibiae were isolated from E15.5 mice, measured and incubated in media containing α-MEM, 5% bovine serum albumin, 1% L-glutamine, and 1% penicillin/streptomycin [22, 23]. The following day, media were changed and inhibitors were added to the culture (DMSO or ethanol vehicle, 10 μM Y27632, 1 μM cytochalasin D, 50 nM jasplakinolide, 10 μM cholesterol, 10 mM (2-hydroxypropyl)-β-cyclodextrin [HPCD; Sigma] and/or 5 μM lovastatin [Sigma]). A subset of organ cultures were pre-treated with 10 mM HPCD and after 4 hrs and then washed in phosphate buffered saline (PBS). The remaining treatments were added every other day to cultures, and after 6 days tibiae were measured and fixed in 4% paraformaldehyde (PFA) overnight at 4°C. Subsets of bones were labelled with BrdU for a period of 4 hrs before being fixed in 4% PFA. Another subset of bones was stained in Alcian Blue/Alizarin Red solution, and the rest were sent for embedding in paraffin and sectioning (Robarts Research Institute, Molecular Pathology, London, Ontario, Canada).

Col2-Cre Rac1$^{fl/fl}$ mice were maintained and genotyped and tibiae were isolated on P0 and sent for sectioning as described [24].

Primary cultures

Long bones (humerus, radius, ulna, tibia, fibula and femur) were isolated from E 15.5 mice and digested in 1 mg/ml of Collagenase P in DMEM containing 10% FBS for 1 hr at 37°C with gentle agitation [15]. Chondrocytes were centrifuged for 5 min. at 1000 rpm and resuspended in media containing 60% F12, 40% DMEM, 10% FBS, 1% L-glutamine and 1% penicillin/streptomycin. Chondrocytes were plated at a density of 500,000 cells/well in a six-well dish (Nunc-Thermo Fisher Scientific; Rochester, NY, USA). After 24 hrs, cultures were treated with 10 μM Y27632, 1 μM cytochalasin D or 50 nM jasplakinolide. After another 24 hrs of incubation with inhibitors, cells were harvested for RNA. Specific chondrogenic gene expression has been previously

For cholesterol studies, primary cultures were isolated as described above, but after an 8-hr culture period, cells were serum-starved. After 24 hrs in serum-free medium, subsets of cells were pre-treated with 10 mM HPCD (Sigma) for a period of 4 hrs. After a wash-out, cells were then treated with either DMSO (vehicle), ethanol (vehicle), 1 μM cytochalasin D, 5 μM lovastatin, or 10 μM cholesterol in serum free medium. After another 24-hr period, cells were harvested for RNA isolation.

Microarray analysis

Chondrocytes were isolated as above, plated in high-density monolayer and treated for a period of 24 hrs with DMSO for control, 10 μM Y27632, 1 μM cytochalasin D or 50 nM jasplakinolide. RNA was isolated using the RNeasy kit (QIAGEN, Mississauga, Ontario, Canada) and then sent for assessment of quality with Agilent 2100 BioAnalyzer Data Review Software

(Wilmington, DE, USA) at the London Regional Genomics Center before hybridization to Affymetrix430A (Santa Clara, CA, USA) chips (Robarts Research Institute, London, Ontario, Canada). Raw data were analysed by GeneSpring 7.3.1, and gene lists were compiled from probe sets demonstrating a reliable signal as determined by M.A.S. 5.0 derived algorithms followed by a one-way Welch ANOVA (*P*-value cut-off of 0.05). Probe set lists were filtered using the 'Filter on Fold Change' option in GeneSpring. A minimum 1.5-fold change in gene expression was implemented, in comparison of DMSO control treated RNA samples to samples treated with inhibitors, as described [13, 25].

Potential Ror-α targets were determined with the mouse genome9999 application from GeneSpring. The list of probe sets up-regulated by cytochalasin D were translated into the genome9999 application, and 506 probe sets of the 777 originally identified gene list were scanned over the 5000 base pairs upstream for the transcriptional start sites for the RORE consensus sequence ANNTAGGTCA [26], as described [25]. A total of 103 probe sets contained the consensus sequence, only exact matches are listed.

RT real-time PCR

RNA was isolated from primary cultures using the RNeasy kit (QIAGEN) as per manufacturers' protocol. Twenty-five nanograms of RNA were plated per well in quadruplicate. Relative gene expression was determined measuring *Rora*, lymphocyte cystolic factor 1 (*Lcp1*), *Osteoadherin*, frizzled related protein (*Frzb*), *Gdf10*, aldehyde dehydrogenase family 1, subfamily A3 (*Aldh1a3*), fatty acid binding protein 4 (*Fabp4*), kruppel-like factor 5 (*Klf15*) (Assays on demand, Applied Biosystems; Forest City, CA, USA) relative to glyceraldehyde-3-phosphate dehydrogenase (*Gapdh*) using one step RT qPCR Master Mix (Applied Biosystems) and 40 cycles on the ABI prism 7900 HT sequence detector (PerkinElmer Life Sciences; Waltham, MA, USA) as described [27, 28].

Immunohistochemistry

Sections were dewaxed in xylene and rehydrated in serial ethanol washes. Endogenous peroxidases were blocked by incubating tissues in 3% hydrogen peroxide in methanol for 30 min. Antigen retrieval was performed by boiling samples in 0.1 M sodium citrate/PBS solution, pH 6, for 20 min. followed by rinsing in double distilled water. After blocking sections for 30 min. at room temperature in appropriate animal serum:PBS (1:20), primary antibodies were diluted 1:200 in the blocking solution and incubated overnight at 4°C. The following day, tissue sections were rinsed in PBS and incubated with appropriate HRP-conjugated secondary antibodies, 1:200 diluted in PBS for 1 hr. Sections were washed in PBS and then incubated with Diaminobenzidine (Dako, Mississauga, ON, Canada) for colorimetric detection.

Statistical analysis

Longitudinal growth of long bones are the average of five independent experiments, with six tibia per trial, the mean longitudinal growth $\pm$ S.E.M. Data were analysed by one-way ANOVA followed by a post Bonferroni test.

RNA used for real-time PCR analyses were collected from three independent trials (long bones collected from the embryos of one or two litters) and run in quadruplicate. The data shown are the average mean gene expression of three independent trials, normalized to the vehicle control cultures $\pm$ S.E.M. Data were analysed by one-way ANOVA followed by a *post hoc* Bonferroni test.

Results

Disruption of actin organization increases longitudinal growth of organ cultures and alters growth plate organization

We wanted to determine the effects of modifying the actin cytoskeleton on chondrocytes in the three dimensional environment of the growth plate. Tibiae isolated from E15.5 mice were incubated with DMSO vehicle, 10 μM Y27632 (which inhibits Rho/ROCK signalling), 1 μM cytochalasin D (an inhibitor of actin polymerization) or 50 nM jasplakinolide (stabilizes and promotes actin polymerization). After 6 days in culture, bones were stained with alcian blue/alizarin red to assess glycosaminoglycan production and mineralization, respectively. Bones treated with Y27632 grew slightly longer and appeared to have less alizarin red stain, indicating less mineralization (Fig. 1A). Bones treated with either cytochalasin D or jasplakinolide were markedly larger than controls (Fig. 1A). Quantitative measurements of treated bones demonstrate significant increases in longitudinal growth compared to control cultures (Fig. 1B).

We next asked how growth plate architecture was affected by these treatments by staining paraffin sections with haematoxylin. The resting (green arrow), proliferative (blue arrow) and hypertrophic (black arrow) zones of control growth plates were clearly distinguished in control bones (Fig. 1C). Growth plate zone measurements revealed that inhibition of ROCK signalling by Y27632 results in an expanded resting zone, whereas the proliferative and hypertrophic zones sizes remain unchanged (Fig. 1D). Interestingly, the proliferative zone is hypocellular in Y27632 treated bones, suggesting an effect on chondrocyte proliferation. Tibiae treated with jasplakinolide showed significantly expanded resting, proliferative and hypertrophic zones (Fig. 1D). Inhibition of actin polymerization by cytochalasin D resulted in a growth plate that was too unorganized to distinguish and measure any zones (Fig. 1D). Instead, the cellular morphology of cytochalasin D treated tibiae showed features of hypertrophic and resting chondrocytes; cells were larger but were also surrounded by an abundant matrix.

Because all treatments resulted in increased longitudinal growth as compared to the control, we examined the effect of these treatments on cell proliferation using BrdU labelling. Control growth plates label with BrdU mostly in the proliferative region of the growth plate, with some positive cells in the resting zone (Fig. 1E). Bones treated with Y27632 or jasplakinolide displayed a slight increase in BrdU labelling; however, the pattern of labelling extended into the upper portion of the hypertrophic zone and more cells were labelled in the resting zone (Fig. 1E),

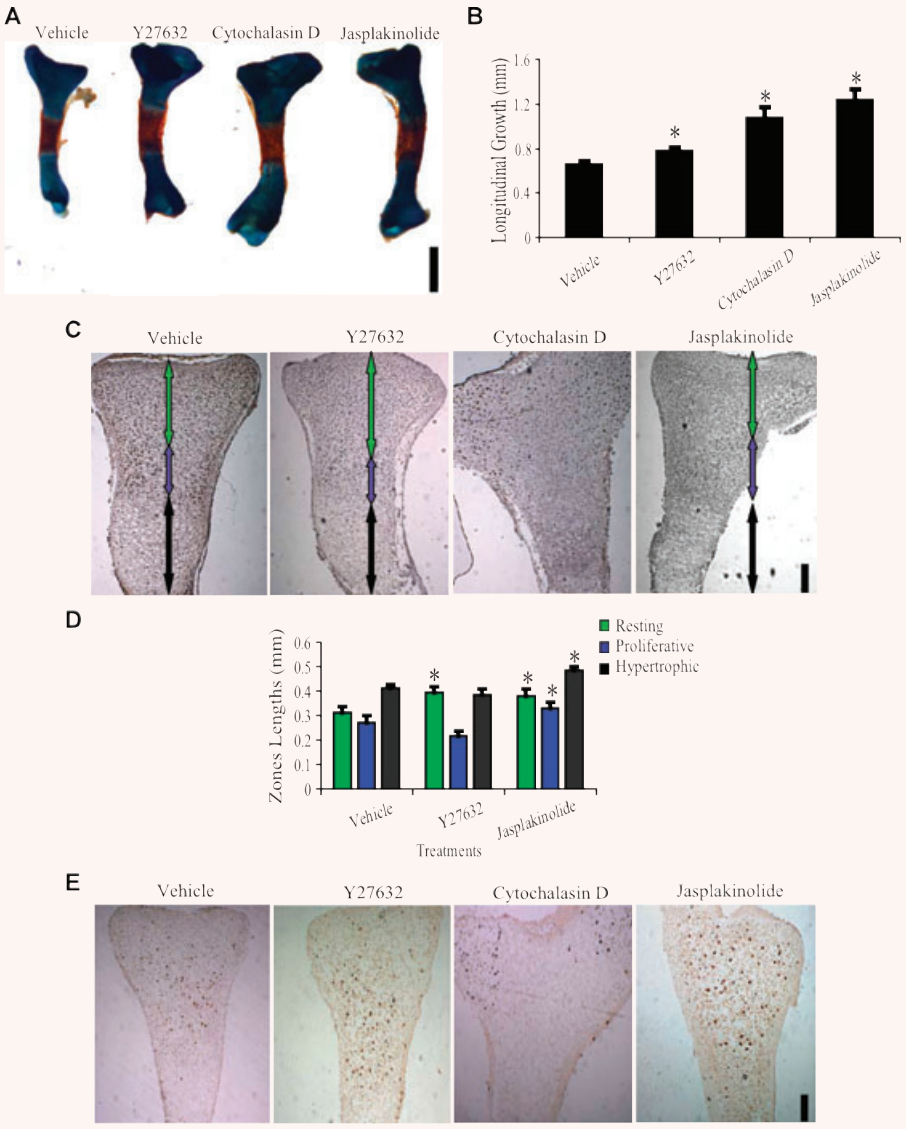

Fig. 1 Disruption of actin organization increases bone growth in organ culture and alters growth plate organization. Tibiae were isolated from E15.5 mice and incubated for a period of 6 days with DMSO vehicle, 1 μM cytochalasin D, 10 μM Y27632 or 50 nM jasplakinolide. (**A**) Tibiae were fixed and then stained with Alcian Blue for the detection of sulphated glycosaminoglycans and with Alizarin Red for mineral content. Data shown are representative of four independent trials, scale bar = 1 mm. (**B**) Lengths of tibiae were measured at the beginning and end of the 6-day culture period to determine the average longitudinal growth. All treatments result in a significant increase in longitudinal growth, but both cytochalasin D and jasplakinolide resulted in a dramatic increase in both longitudinal and appositional growth. Data shown are the average of five independent experiments, with six tibia per trial, the mean longitudinal growth ± S.E.M., $*P < 0.05$. (**C**) A subset of tibia were fixed, dehydrated, embedded in paraffin and sectioned for histological analysis of growth plate organization. Sections were stained with haematoxylin and eosin for visualization of basic histology. Data shown are representative of four independent trials, scale bar = 0.1 mm. (**D**) Growth plate zones were measured on the basis of cellular morphology and organization of histological sections by a blind observer. Data shown are the average of four independent experiments, four bones per trial, the length ± S.E.M., $*P < 0.05$. (**E**) Tibiae were grown in culture for a period of 6 days in the presence of vehicle, 10 μM Y27632, 1 μM cytochalasin D or 50 nM jasplakinolide. At the end of the culture period, tibiae were incubated in media containing BrdU for 4 hrs and then washed in PBS. Bones were fixed, dehydrated and embedded in paraffin, followed by sectioning and then immunohistochemistry for BrdU. Data shown are representative, scale bar = 0.1 mm.

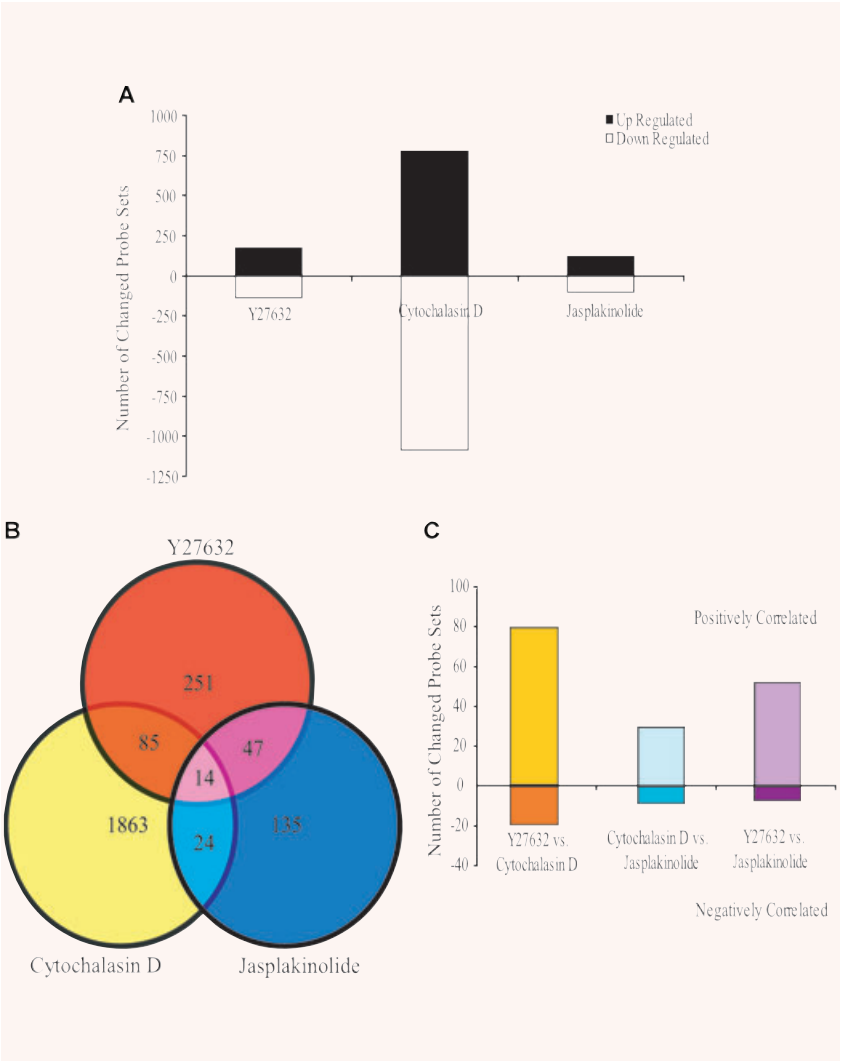

Fig. 2 Microarray analysis of primary chondrocytes treated with actin inhibitors. An enriched population of primary mouse chondrocytes were treated with DMSO vehicle, 1 μM cytochalasin D, 10 μM Y27632 or 50 nM jasplakinolide for 24 hrs. RNA was isolated and hybridized to Affymetrix MOE 4.0 chips. Gene lists were compiled from genes that demonstrated a reliable signal (as determined by the MAS5.0 algorithm) and changed significantly; a 1.5-fold cut-off was assigned. (**A**) Inhibition of Rho/ROCK signalling by Y27632 resulted in 176 probe sets being up-regulated and 139 probe sets being down-regulated. Cytochalasin D treatment resulted in 777 up-regulated and 1209 down-regulated probe sets in comparison to control cultures while jasplakinolide treatment resulted in 120 probe sets being up-regulated and 107 probe sets being down-regulated. (**B**) Comparisons of all probe sets regulated by the three different pharmacological actin modifiers demonstrate that 14 probe sets are commonly regulated by all treatments. A total of 85 probe sets are commonly regulated by both Y27632 and cytochalasin D, 24 probe sets are commonly regulated by cytochalasin D and jasplakinolide and 47 probe sets are commonly regulated by Y27632 and jasplakinolide. (**C**) Commonly regulated probe sets were assessed for positive or negative correlation between treatments. Probe sets that were up-regulated or down-regulated by both treatments were assigned a positive correlation, while probe sets that were up-regulated in one treatment and down-regulated in the other were assigned a negative correlation. The majority of probe sets were positively correlated in all treatments.

suggesting deregulation of cell cycle progression under these conditions. Cytochalasin D-treated bones did not have an organized growth plate, but the area in which the proliferative zone should reside had no cells positively labelled with BrdU. Instead, a few cells on either side of the upper condyle were labelled by BrdU (Fig. 1E). These data suggest that bones treated with cytochalasin D do demonstrate enhanced proliferation but in the resting growth plate zone which is uncharacteristic of normal growth plates, possibly contributing to the enhanced growth observed.

Microarray analysis of primary embryonic growth plate chondrocytes treated with actin inhibitors

We wanted to assess global changes of gene expression in chondrocytes in response to actin modulators to gain insights into the molecular pathways mediating the observed responses. RNA from a mixed population of primary mouse chondrocytes were isolated from embryonic long bones (as described by [22]) treated with the various compounds was hybridized to Affymetrix microarrays representing the entire mouse genome. Inhibition of ROCK signalling by Y27632 treatment resulted in significant up-regulation of 176 probe sets, and down-regulation of 139 probe sets (Fig. 2A, Table S1). Cytochalasin D treatment induced up-regulation of 777 probe sets and down-regulation of 1209 probe sets (Fig. 2A, Table S2). Stimulation of actin polymerization by jasplakinolide treatment resulted in 120 probe sets being up-regulated and 107 down-regulated (Fig. 2A, Table S3).

We wanted to determine whether the different treatments regulated a common set of genes. We compared gene lists and determined that 14 probe sets were regulated in all three (Fig. 2B); 12 probe sets corresponded to genes listed in Table 1. Y27632 and cytochalasin D treatment were the most similar with 99 common probe sets while jasplakinolide regulated 61 common genes

Table 1 Probe sets commonly regulated by all compounds tested gene name gene description

		Fold change		
		CytD	Y27632	Jasp
Acaa1b	3-ketoacyl-CoA thiolase B	−7.6	2.0	−1.9
Actg2	Actin, γ_2, smooth muscle, enteric	6.4	−1.9	5.3
Aspm	Calmodulin binding protein 1	−2.0	−2.0	−2.4
Cnn1	Calponin 1	3.6	−2.8	3.3
Ereg	Epiregulin	−1.9	−2.3	1.9
Gjb2	Gap junction membrane channel protein β_2	−6.1	−3.1	1.6
Lcp1	Lymphocyte cytosolic protein 1	4.7	1.5	1.7
Mylk	Myosin, light polypeptide kinase	4.1	2.6	2.3
Osr1	Odd-skipped related 1 (*Drosophila*)	−5.3	−1.7	−1.9
Wdr33	WD repeat domain 33	−1.8	2.1	−2.6
Depdc6	DEP domain containing 6	−2.3	2.0	1.7
Rtel1	Regulator of telomere elongation helicase 1	−1.9	−1.6	−1.7

with Y27632 and 38 with cytochalasin D. The majority of probe sets common to two of the inhibitors tested were positively correlated; for example, if up-regulated by one inhibitor, it was also up-regulated by the other compound (Fig. 2C). Cytochalasin D and jasplakinolide are often regarded as having opposing effects because one inhibits whereas the other promotes actin polymerization [29, 30]. However, many genes commonly regulated by both compounds were positively correlated (Fig. 2C). This is not without precedent as the regulation of transcription or the activity of some genes/proteins appear to be responsive to changes in actin dynamics and not specifically to either inhibition or polymerization of actin, such as Sox9 and the serum response factor (SRF) [14, 31].

Pathways and processes regulated by cytochalasin D treatment

We analysed the data set of cytochalasin D treatment in more detail because this compound elicited the most dramatic changes both in gene expression and growth of tibia organ cultures. The gene list generated from cytochalasin D treatment compared to DMSO treated chondrocytes was analysed for molecular function by Fatigo+ software (Babelomics http://babelomics2.bioinfo.cipf.es/index.html) [32]. We show that a large proportion of regulated genes are involved in nucleic acid metabolism, including 215 probe sets in the category of nucleic acid binding, 62 transcription factors and 15 in chromatin binding. Other interesting categories included lipid binding and lipid transport with 34 and 5 probe sets, respectively (Fig. 3A).

Next we identified common signalling pathways between genes that changed in response to cytochalasin D treatment using Kegg pathway analyses (Babelomics). We found that cell cycle regulation was the category most responsive to cytochalasin D, with 32 down-regulated and only 2 up-regulated probe sets, in agreement with the decrease in BrdU labelling observed earlier (Fig. 3B). Four specific signalling pathways were identified; transforming growth factor-β signalling, Wnt signalling, mTOR signalling and PPAR signalling, all of which have been previously implicated in the regulation of endochondral bone growth [33–36].

Gene ontology and KEGG analyses were also performed for the other two treatments (Figs. S1 and S2). Of note, Y27632 treatment strongly down-regulated several genes involved in cytokine signalling, whereas the most pronounced effect of jasplakinolide was up-regulation of genes involved in actin regulation, focal adhesions, ECM receptor interactions and cell communication.

Comparison of cytochalasin D effects to gene expression patterns during chondrocyte differentiation *in vitro* and *in vivo*

We had shown that organ cultures treated with cytochalasin D displayed a completely disorganized growth plate consisting of large cells, similar in morphology to hypertrophic chondrocytes. Due to this observation, we compared genes up-regulated in cytochalasin D treatment to genes up-regulated in the hypertrophic growth plate of microdissected bones and genes up-regulated during hypertrophic differentiation of micromass cultures [13] (Fig. 4). Of the 777 probe sets up-regulated in cytochalasin D treatment, almost 50% are up-regulated during hypertrophy in one or both of these models, suggesting that cytochalasin D induces selective features of hypertrophy, in agreement with the cellular appearance. A total of 56 probe sets are common to all three models and are listed (Table 2). These genes included *Rora and Lcp1*. Other genes of interest include *Frzb* and *Gdf10* which were commonly up-regulated by cytochalasin D treatment and in hypertrophic microdissected bones, but not in the micromass culture system.

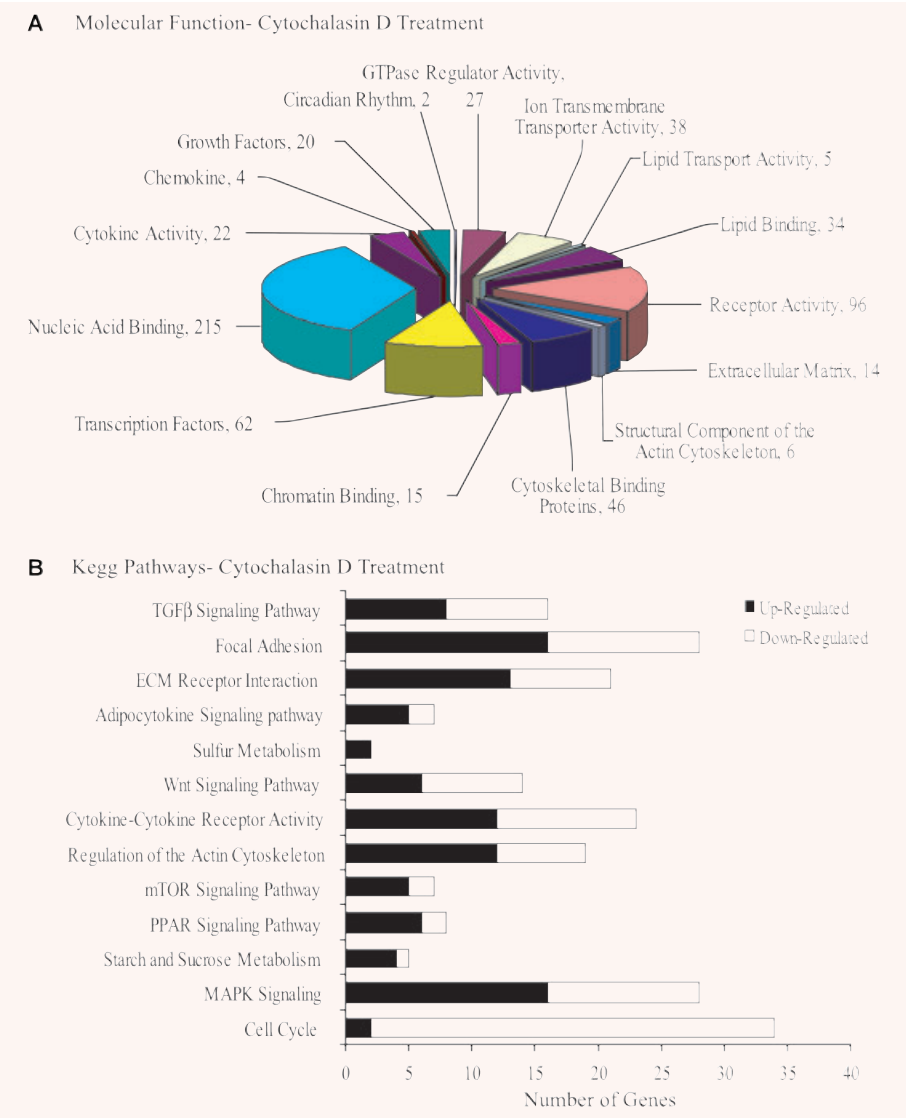

Fig. 3 Gene ontology and Kegg pathways in response to cytochalasin D treatment. (**A**) Microarray gene sets from primary chondrocytes treated with 1 μM cytochalasin D for a period of 24 hrs were assessed according to GO annotations categorized by Fatigo+. (**B**) Kegg annotations were used to determine changes within different signalling pathways.

Real-time validations of selected genes changing in response to actin inhibitors

We next confirmed regulation of selected genes from our microarray data by real-time PCR. The gene encoding the nuclear receptor *Rora* was increased by cytochalasin D treatment in the microarray. Here we confirmed that mRNA levels of *Rora* are significantly increased in response to cytochalasin D treatment but also in response to jasplakinolide, whereas Y27632 reduced *Rora* transcript levels (Fig. 5A). *Lcp1* was up-regulated by all three inhibitors in the microarray. Real-time PCR validated that cytochalasin D, Y27632 and jasplakinolide treatment result in significant increases of *Lcp1* mRNA levels (Fig. 5B). The Wnt antagonist Frzb has been previously identified as a promoter of endochondral ossification and was up-regulated in response to cytochalasin D treatment in the microarray [37]. *Frzb* mRNA levels were significantly increased in response to cytochalasin D treatment as compared to controls in real-time PCR (Fig. 5C). *Gdf10* is part of the transforming growth factor-β family and is closely related to *Gdf5*, a gene known to be important in cartilage differentiation [38]. Furthermore, another study has shown that Gdf10 may be important for regulation of cell differentiation in skeletogenesis due to its expression pattern in calvaria and long bones [39]. *Gdf10* was shown to be up-regulated by both cytochalasin D and Y27632 treatment in the microarray. Real-time PCR analyses confirmed these data and showed that both treatments result in significantly increased mRNA levels of *Gdf10* (Fig. 5D). Ror-α was selected for follow up studies due to it's response to various actin modifications,

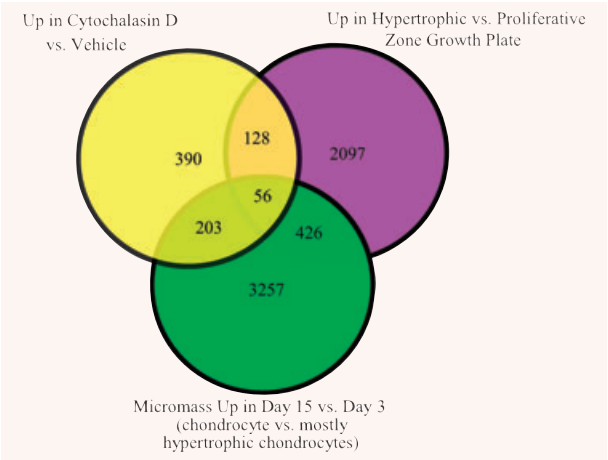

Fig. 4 Comparison of cytochalasin D treatment to hypertrophic gene expression *in vivo* and *in vitro*. Microarray data sets from three different experiments were compared: (1) RNA was isolated from an enriched population of primary chondrocytes plated in high-density monolayer cultures and treated for a period of 24 hrs with DMSO vehicle or 1 μM cytochalasin D. (2) RNA was isolated from micromass cultures of differentiating chondrocytes on day 3 and day 15 of culture. (3) RNA was isolated from E15.5 tibiae that were microdissected into different growth plate zones. All experiments were run in triplicate for each treatment or time-point. RNAs were hybridized to Affymetrix chips for the micromass arrays we used different chips, raw data were imported into Genespring7.3.1 and gene lists were generated from those probe sets that demonstrate a reliable signal as determined by M.A.S. 5.0 and that changed significantly as determined by a one-way ANOVA. A cut-off of 1.5-fold change was implemented and those probe sets that were significantly up-regulated by 1.5-fold in cytochalasin D treatment *versus* DMSO control, 1.5-fold up-regulated in the hypertrophic region of the growth plate *versus* the resting zone and 1.5-fold up-regulated on day 15 of micromass culture *versus* day 3 of culture were compared. A total of 56 probe sets were commonly regulated in all three models. A total of 426 probe sets were commonly regulated in the microdissected hypertrophic growth plate *versus* the differentiated micromass culture. A total of 203 probe sets were commonly regulated in differentiated micromass culture and cytochalasin D treatment and 128 probe sets were commonly regulated in the cytochalasin D treatment *versus* the hypertrophic growth plate.

as well for its known role in lipid metabolism, an important functional category identified in our micorarray analyses in response to actin dynamics.

Expression of Ror-α in the growth plate

We analysed the expression pattern of Ror-α protein (the product of the *Rora* gene) within the growth plate of tibia organ cultures. Ror-α is most highly expressed within the pre-hypertrophic/hypertrophic region of the growth plate of control cultures, consistent with the pattern of expression determined in our microarrays (Fig. 6A). When organ cultures were grown in the presence of cytochalasin D, Ror-α expression was found throughout the growth plate (Fig. 6A). These data further suggest that cytochalasin D treatment results in a pre-hypertrophic/hypertrophic-like phenotype in growth plates.

Hif-1α plays an important role in cartilage development [40] and is a direct regulator of Ror-α gene expression in other cell types [41]. Hif-1α gene expression was found to be up-regulated in response to cytochalasin D treatment of primary monolayer chondrocytes in our microarray data set in comparison to controls. We therefore wanted to examine the pattern of expression of Hif-1α in the growth plate to compare its expression to that of Ror-α. In control organ cultures, Hif-1α expression is highest in the pre-hypertrophic and hypertrophic region of the growth plate, consistent with the literature [40] (Fig. 6B). Hif-1α expression is also highly expressed in the periphery of the growth plate with strong expression in the upper portion of the resting zone (Fig. 6B). Cytochalasin D treated organ cultures exhibited Hif-1α expression throughout the growth plate, similar to Ror-α (Fig. 6B). These data suggest that the increase in Ror-α gene and protein expression observed might be due to the effect of cytochalasin D stimulating increased expression of Hif-1α in both the growth plate and primary monolayer culture.

We next complemented our pharmacological approaches using genetic inactivation of a physiological regulator of actin dynamics. Control mice displayed Ror-α and Hif-1α protein expression in pre-hypertrophic and hypertrophic chondrocytes, consistent with the expression pattern observed in tibia organ cultures (Fig. 6C). Mice with cartilage-specific inactivation of the *Rac1* gene, a key regulator of actin organization, display numerous skeletal defects, including disrupted growth plate organization, dwarfism and skeletal deformities [24]. Rac1 deficiency resulted in increased levels of Hif-1α in the hypertrophic region of the growth plate in comparison to control bones (Fig. 6C) and a similar increased area of Ror-α expression (Fig. 6C), suggesting that genetic disruption of actin organization *in vivo* also results in increased expression of Hif-1α and Ror-α.

Functional validations of genes up-regulated by cytochalasin D

There is evidence from the literature that Ror-α is no longer an orphan receptor as two potential ligands have been discovered, melatonin and cholesterol (as well as cholesterol sulphate) [42, 43]. Bioinformatics analyses suggested that cytochalasin D treatment of chondrocytes affected a large number of known or putative target genes of Ror-α (Table 3). We therefore wanted to assess if these genes are regulated by cholesterol in primary monolayer chondrocytes. Chondrocytes were treated with either cytochalasin D or vehicle control. To inhibit endogenous Ror-α activity in either of these treatments, we pre-treated a subset of these cells with HPCD (to block intracellular transport of cholesterol) and lovastatin (to inhibit cholesterol synthesis through the mevalonate pathway) [44]. Additional subsets of these cells were

Table 2 Probe sets commonly regulated by cytochalasin D and models of hypertrophy. (1) Genes (probe sets) up-regulated by cytochalasin D in comparison to DMSO vehicle (CytD), (2) Genes (probe sets) up-regulated in the hypertrophic zone in comparison to the resting/proliferative zone (GP) and (3) Genes (probe sets) up-regulated in the micromass culture system, day 15 in comparison to day 3 of culture (MM).

Gene name	Gene description	Fold change		
		CytD	GP	MM
1110018J18Rik	RIKEN cDNA 1110018J18 gene	2.0	1.9	1.9
1810054D07Rik	RIKEN cDNA 9130422G05 gene	2.5	20.5	3.0
		2.1	4.3	2.4
3110005G23Rik	RIKEN cDNA 3110005G23 gene	1.6	3.0	1.7
4930471M23Rik	RIKEN cDNA 4930471M23 gene	1.8	1.9	2.0
Agt	Angiotensinogen	10.9	2.5	2.1
Ak3l1	Adenylate kinase 4	3.4	3.4	1.8
		3.2	3.3	1.5
Anxa11	Annexin A11	2.2	3.7	1.6
Anxa4	Annexin A4	1.7	3.2	4.3
Atf3	Activating transcription factor 3	9.6	2.3	2.7
Bnip3	BCL2/adenovirus E1B 19kDa-interacting protein 1, NIP3	3.5	1.6	2.7
Camk1	Calcium/calmodulin-dependent protein kinase I	1.9	1.8	1.8
		1.9	1.7	1.7
Chac1	Cation transport regulator-like 1 (*E. coli*)	2.5	2.4	1.7
Cth	Cystathionase (cystathionine γ-lyase)	4.3	1.7	2.9
Eps8l2	EPS8-like 2	2.1	2.1	1.5
F13a1	Coagulation factor XIII, alpha subunit	3.2	3.4	6.2
Fuca2	RIKEN cDNA 0610025O11 gene	1.7	1.6	2.3
Gba	Glucosidase, β; acid	2.0	1.9	1.6
Hist2h2aa1	Histone 2, H2aa1	2.5	1.6	1.6
Htatip2	HIV-1 tat interactive protein 2, homolog (human)	2.2	4.6	6.6
Il16	Interleukin 16	4.5	2.1	2.7
Jam2	Junction adhesion molecule 2	3.4	1.7	1.6
Lcp1	Lymphocyte cytosolic protein 1	8.9	4.4	20.2
		4.6	2.6	8.7
Leprotl1	Leptin receptor overlapping transcript-like 1	2.0	1.6	2.5
Lpl	Lipoprotein lipase	2.2	1.9	23.0
Mid2	Midline 2	6.9	2.5	2.4
Mras	Muscle and microspikes RAS	2.6	4.3	1.6
Myo6	Myosin VI	2.3	5.7	1.8
Ndg2	Nur77 downstream gene 2	5.0	2.1	2.2
Ndrg1	N-myc downstream regulated 1	2.9	1.5	15.0

Continued

Table 2 Continued

Gene name	Gene description	Fold change		
		CytD	GP	MM
Neu1	Neuraminidase 1	2.5	1.6	2.3
Nupr1	Nuclear protein 1	3.4	4.8	7.5
		3.1	4.3	5.9
Pde8a	Phosphodiesterase 8A	2.6	4.2	1.6
Pfkp	Phosphofructokinase, platelet	2.9	1.5	2.6
Pim3	Proviral integration site 3	2.3	2.6	1.6
Plxnd1	Plexin D1	2.7	1.9	2.1
Ppp1r1b	Protein phosphatase 1, regulatory (inhibitor) subunit 1B	5.6	4.9	2.0
Psph	Phosphoserine phosphatase	2.2	2.4	1.8
Rgs3	Regulator of G-protein signalling 3	1.8	3.1	3.3
Rora	RAR-related orphan receptor-α	4.0	1.6	3.6
		3.3	1.6	2.4
Scarb2	Scavenger receptor class B, member 2	2.3	2.8	2.1
Serinc3	Tumour differentially expressed 1	2.1	2.5	2.0
Slc1a3	Solute carrier family 1, member 3	1.8	2.3	1.9
Slc35a3	Solute carrier family 35 (UDP-N-acetylglucosamine (UDP-GlcNAc) transporter), member 3	2.7	2.0	1.6
Slc7a2	Solute carrier family 7 (cationic amino acid transporter, y + system), member 2	2.6	1.9	1.8
Stc2	Stanniocalcin 2	21.6	1.7	4.2
Steap1	Six transmembrane epithelial antigen of the prostate	2.8	5.7	3.5
Steap3	Steap family member 3	2.5	1.7	8.9
Tgfb1	Transforming growth factor, β_1	2.3	2.0	2.6
Tgoln1	Trans-golgi network protein	1.9	2.2	1.6
Trpv4	Transient receptor potential cation channel, subfamily V, member 4	2.0	1.6	1.6

then given exogenous cholesterol to see if the effects of cholesterol inhibitors could be rescued. We first examined the effects of these treatments on baseline *Rora* gene expression. *Rora* gene expression was not affected by either; decreased or increased levels of cholesterol (Fig. 7A). Cytochalasin D treatment resulted in an increase of *Rora* mRNA levels (white bars), as shown previously (Fig. 3A), but this increase in response to cytochalasin D (white bars) was not altered when cholesterol synthesis was inhibited (column set 3) or exogenous cholesterol was added (column set 4) (Fig. 7A).

Lipoprotein lipase (*Lpl*) is a known target of Ror-α signalling and is involved in lipid homeostasis [45]. We show that cytochalasin D treatment increases *Lpl* mRNA levels (white bar, column 1) but the inhibition of cholesterol synthesis (black bar, column 3) resulted in a significant decrease of basal *Lpl* mRNA levels and a complete block of cytochalasin D induction (white bar, column 3) (Fig. 7B). Addition of exogenous cholesterol (black bar, column 4) was able to overcome this deficiency and markedly increased basal *Lpl* mRNA levels, without further induction by cytochalasin D (white bar, column 4) (Fig. 7B). *Fabp4* is a confirmed target gene of Ror-α in other cell types and a known regulator of lipid homeostasis [45]. Additionally, *Fabp4* gene expression was increased in response to cytochalasin D treatment in the microarray and confirmed by real-time PCR (white bar, column 1) (Fig. 7C).

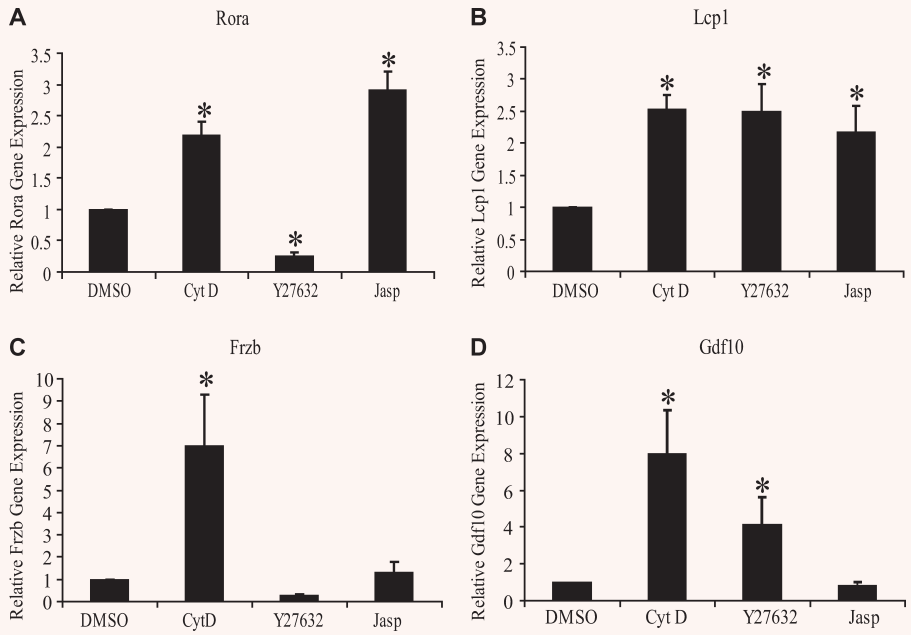

Fig. 5 Real-time validations of selected genes changing in response to actin inhibitors RNA isolated from an enriched population primary chondrocytes plated in high-density monolayer for a period of 24 hrs with vehicle control, 1 μM cytochalasin D, 10 μM Y27632 or 50 nM jasplakinolide were assessed by real-time PCR. (**A**) *Rora* mRNA levels are significantly increased by both cytochalasin D and jasplakinolide treatment in comparison to the vehicle control. Y27632 treatment results in a significant decrease in *Rora* mRNA levels. (**B**) *Lcp1* mRNA levels are significantly increased in response to all treatments in comparison to control cultures. (**C**) Relative gene expression of *Frzb* is significantly increased with cytochalasin D treatment but is unaffected with either jasplakinolide or Y27632 treatment. (**D**) *Gdf10* mRNA levels are significantly increased with both cytochalasin D and Y27632 treatment. Data shown are the average of three independent trials run in quadruplicated, the relative gene expression ± S.E., $^*P < 0.05$.

We demonstrate that inhibition of cholesterol synthesis and shuttling does not affect basal *Fabp4* mRNA levels (black bar, column 3) (Fig. 7C). However, blockade of endogenous cholesterol synthesis and shuttling inhibited the stimulation of *Fabp4* expression by cytochalasin D (white bar, column 3) (Fig. 7C), demonstrating a requirement for cholesterol in the *Fabp4* response to cytochalasin D. Addition of exogenous cholesterol to cultures in which cholesterol synthesis was inhibited resulted in a large increase of basal *Fabp4* mRNA levels (black bar, column 4), with only a minor further increase in response to cytochalasin D (white bar, column 4) (Fig. 7C). These data suggest that cholesterol – and thus Ror-α signalling – is required for the chondrocyte response to cytochalasin D.

Cd36 is a cell surface receptor which binds both collagen I and thrombospondin, is involved in fatty acid translocation and has been shown to be up-regulated in osteoarthritic cartilage [46]. Cd36 is also a known target of Ror-α in other cell types [26]. Here we demonstrate that *Cd36* is up-regulated in response to cytochalasin D treatment (white bar, column 1) (Fig. 7D), but inhibition of cholesterol synthesis blocks the response of cytochalasin D (white bar, column 3) similar to *Fabp4*. Exogenous addition of cholesterol to blocked cultures results in a 3.5-fold increase of *Cd36* mRNA levels (black bar, column 4), with no additional effect of cytochalasin D (white bar, column 4) (Fig. 7D).

The product of the *Aldh1a3* gene metabolizes vitamin A in order to produce retinoic acid [47], and *Aldh1a3* expression is also up-regulated in all three array studies, but the *Aldh1a3* gene is not a known target of Ror-α. We confirmed that inhibition of actin polymerization by cytochalasin D results in increased mRNA levels of *Aldh1a3* (white bar, column 1) (Fig. 7E). However, inhibition of cholesterol synthesis did not block the response of *Aldh1a3* transcript levels to cytochalasin D (white bar, column 3) (Fig. 7E). Additionally, exogenous addition of cholesterol did not affect mRNA levels of *Aldh1a3* (black bar, column 4) (Fig. 7E). These data suggest that regulation of *Aldh1a3* is independent of Ror-α signalling and confirms that the observed effects of cholesterol manipulations are specific to Ror-α target genes.

Klf15 encodes a transcription factor involved in adipogenesis and gluconeogensis [48] and was up-regulated in response to cytochalasin D treatment. We confirm increased mRNA levels of *Klf15* in cultures treated with cytochalasin D (white bar, column 1) (Fig. 7F). The cytochalasin D-induced increase in *Klf15* expression

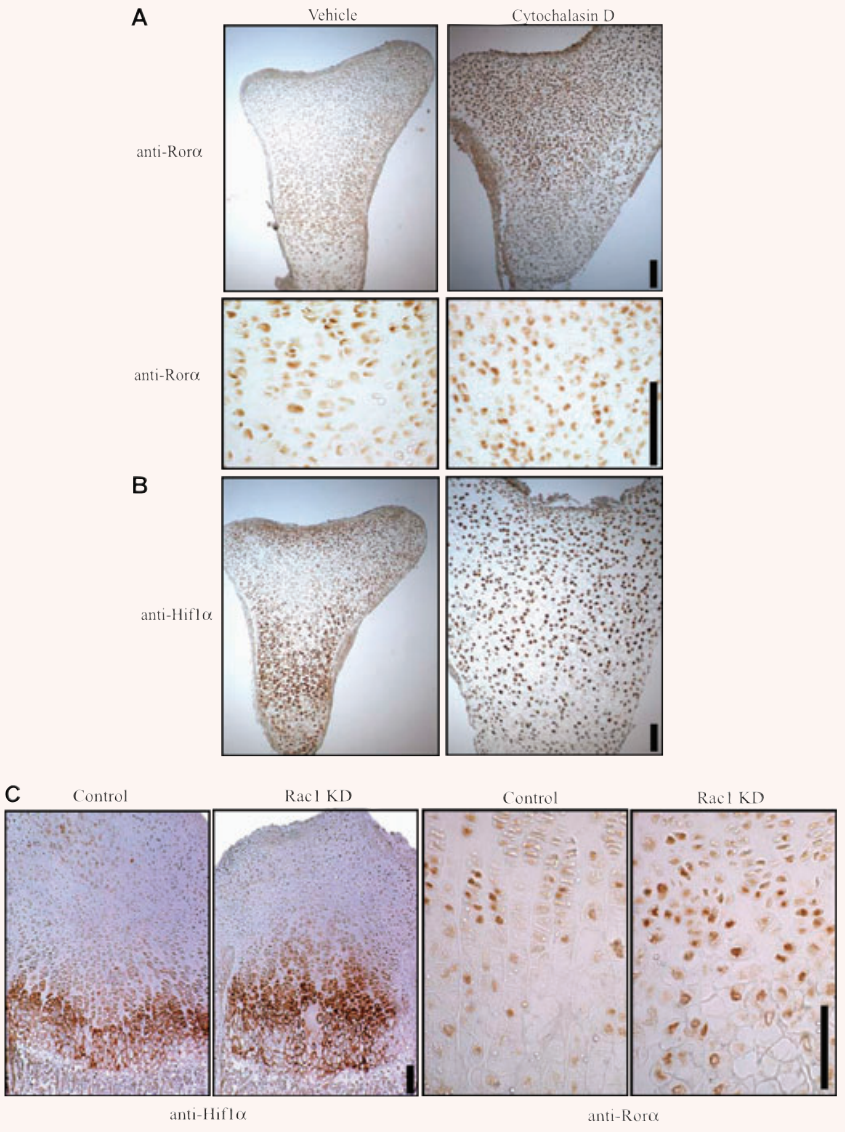

Fig. 6 Ror-α and Hif-1α expression pattern in the growth plate. (**A**) Paraffin-embedded sections from tibia organ cultures were analysed for Ror-α protein expression by immunohistochemistry. Ror-α protein levels are highest in the pre-hypertrophic and hypertrophic regions of control sections, but high throughout the growth plate of cytochalasin D treated bones. Data shown are representative of 3 independent trials, scale bar = 0.1 mm. (**B**) Paraffin embedded sections were analysed for Hif-1α protein expression. Hif-1α protein levels are highest in the pre-hypertrophic and hypertrophic region of control sections. In sections from tibia treated with 1 μM cytochalasin D, Hif-1α expression was found throughout the growth plate. Data shown are representative of 3 independent trials, scale bar = 0.1 mm. (**C**) Tibiae were isolated from newborn control (wild-type) and cartilage-specific Rac1 deficient (knockdown [KD]) animals, Col2-Cre $Rac1^{fl/fl}$ mice. Paraffin embedded sections were analysed for Hif-1α and Ror-α protein expression. Hif-1α protein levels are highest in the lower portion of the proliferative zone and upper portion of the hypertrophic zone. In Rac1 knockdown tibiae, the zone of Hif-1α expression was expanded. Similarly, expression of Ror-α is highest in the pre-hypertrophic region of the growth in control tibiae. The number of cells expressing Ror-α in Rac1 knockdown animals is increased, scale bar = 0.1 mm.

Table 3 Genes up-regulated in response to cytochalasin D containing the Ror-α consensus binding sequence (ANNTAGGTCA)

	RIKEN cDNA 1110007C09 gene
	RIKEN cDNA 1700025G04 gene
	RIKEN cDNA 1810031K17 gene
	RIKEN cDNA 2310031A18 gene
	RIKEN cDNA 3110005G23 gene
	RIKEN cDNA 4933417E01 gene
	RIKEN cDNA 4933426M11 gene
	RIKEN cDNA 9130213B05 gene
	RIKEN cDNA C130038G02 gene
	RNA binding protein gene with multiple splicing
Ank2	Ankyrin 2, brain
Arhgef2	Rho/rac guanine nucleotide exchange factor (GEF) 2
Arl10a	ADP-ribosylation factor-like 10
Armc8	Armadillo repeat containing 8
Aytl2	Acyltransferase like 2
Bambi	BMP and activin membrane-bound inhibitor, homolog (Xenopus laevis)
Bdh	3-hydroxybutyrate dehydrogenase, type 1
Bhlhb2	Basic helix-loop-helix domain containing, class B2
Cd14	CD14 antigen
Col14a1	Procollagen, type XIV, α_1
Col6a3	Procollagen, type VI, α_3
Cpm	Carboxypeptidase M
Cth	Cystathionase (cystathionine γ-lyase)
Ctsb	Cathepsin B
Ddit3	DNA-damage inducible transcript 3
Dirc2	Disrupted in renal carcinoma 2 (human)
Eaf1	ELL associated factor 1
EdnrA	Endothelin receptor type A
Efcab1	EF hand calcium binding domain 1
Efhd1	EF hand domain containing 1
Eif4ebp1	Eukaryotic translation initiation factor 4E binding protein 1
Emp2	Epithelial membrane protein 2
Erf	Ets2 repressor factor
Fabp7	Fatty acid binding protein 7, brain
Fapb4	Fatty acid binding protein 4, adipocyte
Fgfr1	Fibroblast growth factor receptor-like 1
Gadd45a	Growth arrest and DNA-damage-inducible 45 α
Gch1	GTP cyclohydrolase 1
Gdf15	Growth differentiation factor 15
Glt25d2	Glycosyltransferase 25 domain containing 2
Gmppa	GDP-mannose pyrophosphorylase A
Gna13	Guanine nucleotide binding protein, α_{13}
Got1	Glutamate oxaloacetate transaminase 1, soluble
Gpr56	G protein-coupled receptor 56
Gramd1b	GRAM domain containing 1B
Gtl2	GTL2, imprinted maternally expressed untranslated mRNA
Hif1a	Hypoxia inducible factor 1, α subunit
Hist3h2a	Histone 3, H2a
Hr	Hairless
Il11	Interleukin 11
Il16	Interleukin 16
Itga9	Integrin α_9
Jam2	Junction adhesion molecule 2
Lef1	Lymphoid enhancer binding factor 1
Litaf	LPS-induced TN factor
Lrp1	Low-density lipoprotein receptor-related protein 1
Ltbp4	Latent transforming growth factor β binding protein 4
Mbnl2	Muscleblind-like 2
Myd116	Myeloid differentiation primary response gene 116
Myl9	Myosin, light polypeptide 9, regulatory
Nfil3	Nuclear factor, interleukin 3, regulated
Niban	Niban protein
Nog	Noggin
Olfm1	Olfactomedin 1
Olfm1	Phosphoserine phosphatase
P2rx4	Purinergic receptor P2X, ligand-gated ion channel 4
Pdgfrl	Platelet-derived growth factor receptor like
Pigs	Phosphatidylinositol glycan anchor biosynthesis, class S

Continued

Table 3 Continued

Pip5k2c	Phosphatidylinositol-4-phosphate 5-kinase, type II, γ
Ppp1r3c	Protein phosphatase 1, regulatory (inhibitor) subunit 3C
Qpct	Glutaminyl-peptide cyclotransferase (glutaminyl cyclase)
Rab28	RAB28, member RAS oncogene family
Rnf128	Ring finger protein 128
S3—12	Plasma membrane associated protein, S3–12
Satb1	Special AT-rich sequence binding protein 1
Scarb2	Scavenger receptor class B, member 2
Scyl1bp1	SCY1-like 1 binding protein 1
Sel1l	Sel1 (suppressor of lin-12) 1 homolog (C. elegans)
Slc39a6	Solute carrier family 39 (metal ion transporter), member 6
Smoc2	SPARC related modular calcium binding 2
Spink5	Serine peptidase inhibitor, Kazal type 5
Srxn1	Sulfiredoxin 1 homolog (S. cerevisiae)
Tap-1	ATP-binding cassette, sub-family B (MDR/TAP), member 9
Tgfb1	Transforming growth factor, β_1
Tmem144	Transmembrane protein 144
Twsg1	Twisted gastrulation homolog 1 (*Drosophila*)
Vps37b	Vacuolar protein sorting 37B (yeast)
Wif1	Wnt inhibitory factor 1
Wwp2	WW domain containing E3 ubiquitin protein ligase 2
Zfp533	Zinc finger protein 533

was inhibited when cholesterol synthesis is blocked (white bar, column 3), but the blockade could be overcome by exogenous cholesterol (black bar, column 4) (Fig. 7F). These data are reminiscent of those obtained for the known Ror-α target genes *Lpl*, *Fabp4* and *Cd36* and suggest that *Klf15* expression is indeed regulated by Ror-α signalling. Collectively, these data suggest that cytochalasin D effects on selected genes are mediated by cholesterol/Ror-α signalling.

Effects of cholesterol on longitudinal growth and growth plate organization

Our data suggest a role of cholesterol and Ror-α in endochondral bone growth and chondrocyte hypertrophy. To test this hypothesis, tibiae isolated from E15.5 mice were grown for a period of 6 days in the presence of the vehicle control (DMSO or ethanol), 10 μM cholesterol, 1 μM cytochalasin D, and/or pre-treated with HPCD and lovastatin. Tibiae were measured on days 1 and 6 of culture and then fixed and stained with alcian blue/alizarin red. Tibiae treated with cytochalasin D alone were much larger (similar to Fig. 1A) than control organ cultures (Fig. 8A and B). Tibiae that were grown in the presence of cholesterol looked similar to cytochalasin D-treated tibiae (Fig. 8A), but no additive effects of both compounds were observed. When cholesterol synthesis was inhibited by HPCD pre-treatment and lovastatin treatment, tibia growth was significantly inhibited (Fig. 8B). This effect could be rescued by cholesterol but not by cytochalasin D, and both compounds together were not more effective than cholesterol alone. Together, these data demonstrate that cholesterol is required and sufficient to mediate the anabolic effects of cytochalasin D treatment on endochondral bone growth.

Analysis of growth plate organization demonstrated that cholesterol treatment resulted in similar growth plate morphology as cytochalasin D (Fig. 9). Chondrocytes were rounder and larger than control cells; however, cholesterol treatment did not alter growth plate architecture as severely as cytochalasin D treatment because we could still distinguish columnar stacks in the proliferative zone of cholesterol treated bones (Fig. 9). We did notice that the proliferative zone of cholesterol treated bones was hypocellular, suggesting a decrease in chondrocyte proliferation, as found in cytochalasin D treatment (Fig. 9). A combination of cholesterol and cytochalasin D treatment also resulted in larger, rounder chondrocytes. Although some proliferative stacks were seen, this area was hypocellular and disorganized (Fig. 9). Inhibition of cholesterol synthesis by HPCD pre-treatment followed by lovastatin treatment resulted in small, rounded chondrocytes throughout the growth plate. Hypertrophic chondrocytes were also much smaller when cholesterol synthesis was inhibited. Addition of cytochalasin D was unable to rescue the control phenotype (distinctive growth plates zones); however, exogenous cholesterol addition resulted in a more organized growth plate with more clearly defined growth plate zones, as in control cultures (Fig. 9).

Discussion

It has been previously shown that the chondrocyte phenotype is dependent on cellular morphology and the organization of the actin cytoskeleton [49, 50]. The actin cytoskeleton has more functions than only providing cell rigidity, for example in regulating intracellular signalling as well as contributing and modulating cell–cell and cell–matrix interactions [51]. Interestingly, it has been demonstrated that actin binding proteins, such as Filamin A, can be induced to shuttle to the nucleus in response to rearrangement of the actin cytoskeleton and regulate gene expression [52, 53], describing one possible connection between cytoskeletal and cellular phenotype. Here we describe effects on bone growth and global changes in chondrocyte gene expression upon manipulation of the actin cytoskeleton.

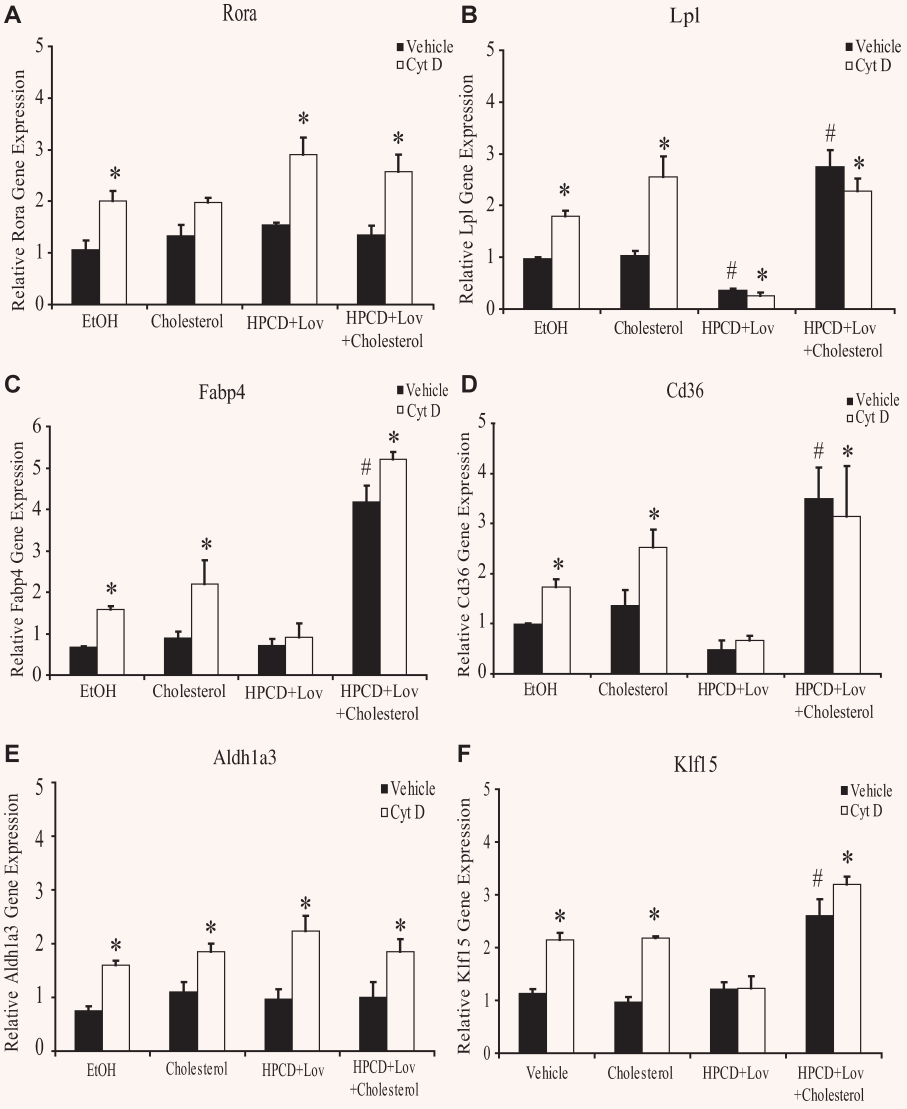

Fig. 7 Functional validations of genes up-regulated by cytochalasin D treatment and some known targets of Ror-α signalling. RNA was isolated from an enriched population of primary chondrocytes plated in high-density monolayer culture that were pre-treated for 4 hrs with 10 mM HPCD or ethanol. After media were changed, cells were treated with vehicle control, 10 μM cholesterol, 5 μM lovastatin and/or 1 μM cytochalasin D. (**A**) *Rora* gene expression was determined by real-time PCR. Cytochalasin D treatment increased mRNA levels of *Rora* independent of increased or decreased levels of cholesterol. (**B**) *Lpl* mRNA levels were significantly increased by cytochalasin D treatment which was inhibited by the addition of HPCD and lovastatin. *Lpl* gene expression was rescued by the addition of cholesterol to HPCD and lovastatin treatment. (**C**) *Fabp4* gene expression is increased with cytochalasin D treatment and this increase was inhibited by HPCD and lovastatin treatment. *Fabp4* gene expression was rescued by the addition of cholesterol. (**D**) *Cd36* gene expression was increased by cytochalasin D treatment and this increase was inhibited by HPCD and lovastatin treatment. The addition of cholesterol in the presence of HPCD and lovastatin resulted in an increase of *Cd36* gene expression. (**E**) *Aldh1a3* is not a known target of Ror-α signalling. *Aldh1a3* gene expression was increased by cytochalasin D treatment but not affected by the inhibition or addition of cholesterol. (**F**) *Klf15* gene expression was significantly increased by cytochalasin D treatment; this increase was inhibited by the treatment of HPCD and lovastatin and then rescued by the addition of cholesterol. Relative gene expression was determined by comparing gene expression to *Gapdh*. Data shown are an average of three independent experiments run in quadruplicate, the mean relative gene expression ± S.E.M., $^{*}P < 0.05$ between the vehicle and cytochalasin D treatment, and $^{\#}P < 0.05$ within the vehicle treatment and the addition or removal of cholesterol.

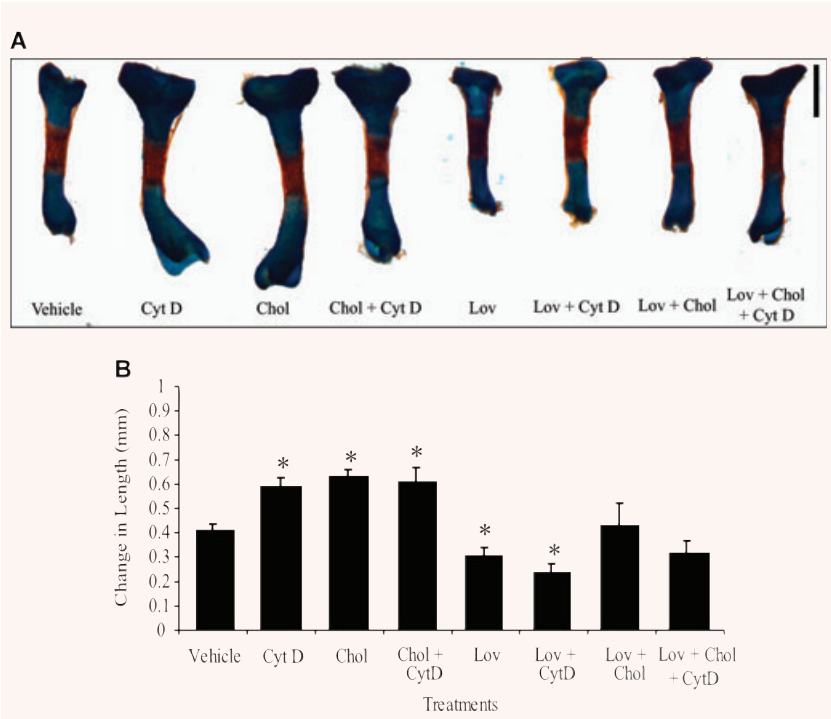

Fig. 8 Longitudinal growth of organ cultures treated with cholesterol and/or inhibition of cholesterol synthesis. (**A**) E15.5 tibiae were grown for a period of 6 days in culture and treated every other day. Subsets of tibiae were pre-treated for a period of 4 hrs with 10 mM HPCD. Remaining tibiae were then treated with vehicle, 1 μM cytochalasin D, 10 μM cholesterol and/or 5 μM lovastatin (HPCD pre-treated tibiae). Bones were fixed and then stained with Alcian Blue/Alizarin Red. Data shown are representative of 3 independent trials, scale bar = 1 mm. (**B**) Tibiae were measured on day 1 of culture and then at the end of 6 days for assessment of longitudinal growth. Tibiae treated with cytochalasin D, cholesterol or a combination of both grew significantly longer than the control. Inhibition of cholesterol signalling by HPCD pre-treatment followed by lovastatin treatment resulted in significantly shorter bones, which could be rescued by exogenous cholesterol but not by cytochalasin D. Data shown are an average of 3 independent trials run in triplicate, ±S.E.M., $^*P < 0.05$.

Inhibition of actin polymerization by cytochalasin D resulted in drastic changes in organ culture growth. Bones treated with cytochalasin D for 6 days were much longer and wider than controls. Upon further examination of growth plate histology, we were unable to distinguish any structure resembling a growth plate, but all cells exhibited enlarged morphology, similar to that of hypertrophic cells. Inhibition of Rho/ROCK signalling and stimulation of actin polymerization by jasplakinolide also resulted in increased longitudinal growth, although analysis of growth plate histology revealed less dramatic changes in structural organization (Fig. 1). Parallel microarray analyses allowed for detailed analysis of the affects of cytochalasin D, Y27632 and jasplakinolide on chondroycte gene expression. In comparison to jasplakinolide treatment, cytochalasin D and Y27632 treatment of primary monolayer chondrocytes resulted in the most similar changes in probe sets; with 99 common genes (Fig. 2B). However, the phenotypic dissimilarity of growth plate organization that was observed is not unexpected because cytochalasin D and Y27632 treatment also regulate 2185 dissimilar probe sets, likely contributing to the disparity in phenotype.

Microarray analysis of chondrocytes treated with actin modifying compounds demonstrated that many genes stimulated by cytochalasin D are known markers of chondrocyte hypertrophy, including *Vegf-α*, *Chondroadherin*, *Mmp3*, *Mmp9* and *Atf3* [27, 54–57]. However, it needs to be noted that other markers of hypertrophy such as type X collagen were not induced significantly by cytochalasin D. Although collagen X is often described as one of the genes expressed during chondrocyte hypertrophy, this does not mean that hypertrophy is not induced in our system. Multiple markers of chondrocyte hypertrophy have been identified and are likely regulated independently of each other and the absence of collagen X is not without precedence [36].

We therefore systematically compared our cytochalasin D data sets to our other microarray studies that examined chondrocyte differentiation *in vitro* [13] or *in vivo* (James *et al.*, in prep.). We found 64 genes that were commonly up-regulated during hypertrophy in these studies and in response to cytochalasin D in the current study, further validating our model that cytochalasin D promotes aspects of chondrocyte hypertrophy. We selected the gene encoding the nuclear receptor Ror-α for follow up studies. Ror-α has been implicated in regulating development of the cerebellum as well as lipid homeostasis, inflammation, and bone maintenance [45, 58–61], but its function in endochondral ossification has not been addressed. We show that Ror-α protein expression is highest in the pre-hypertrophic/hypertrophic region of the growth plate. Furthermore, in cytochalasin D treated bones, *Rora* gene expression is found throughout the entire growth plate. These data suggest that *Rora* gene expression corresponds to hypertrophy and may be a regulator of the terminal stage in chondrocyte differentiation.

Many of the other genes up-regulated in our array in response to cytochalasin D treatment were shown to be involved in lipid signalling and shuttling as well as being known targets of Ror-α signalling. Therefore, we wanted to assess if Ror-α activity was responsible for the increase expression of this subset of genes in our system, by manipulating levels of the Ror-α ligand cholesterol.

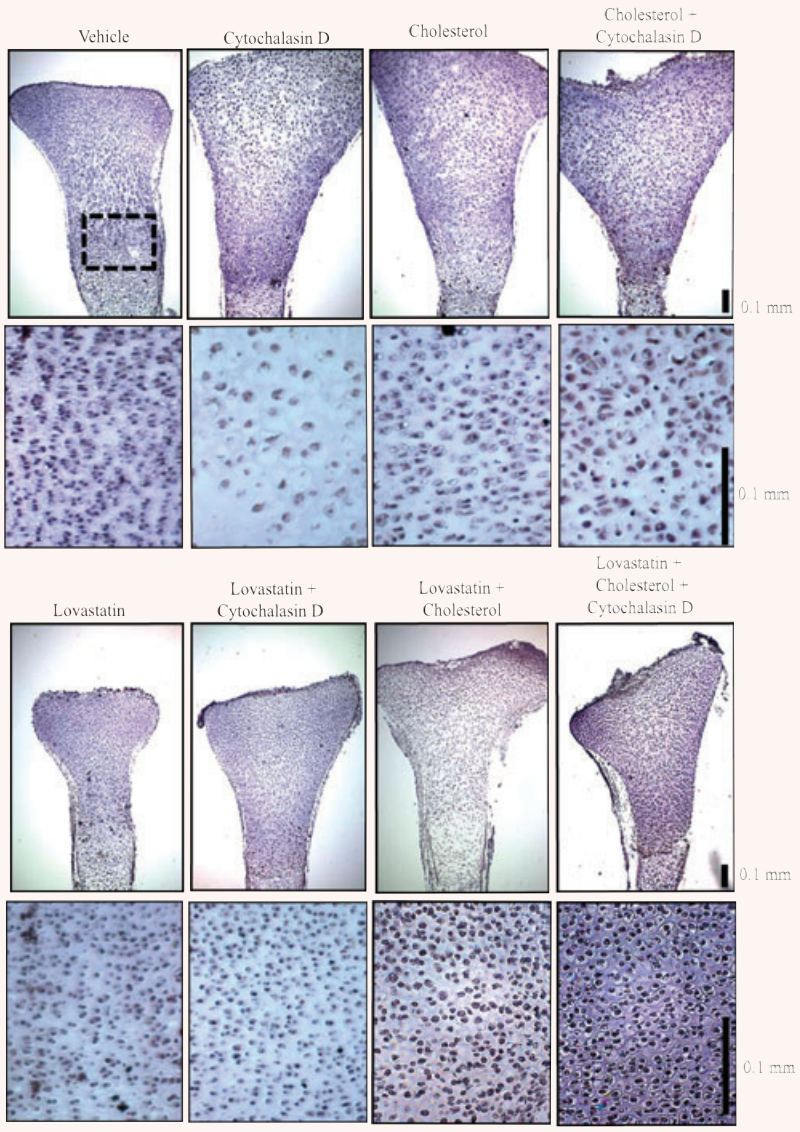

Fig. 9 Growth plate morphology of cholesterol treated tibia. After 6 days in culture, treated tibiae were embedded in paraffin and sectioned. Growth plates were stained with haematoxylin for visualization of growth plate organization. Growth plates were treated with cholesterol and in combination with cytochalasin D or cholesterol synthesis was inhibited by HPCD pre-treatment followed by lovastatin and in combination with cholesterol and cytochalasin D. Growth plates treated with cholesterol showed larger, more rounded cells throughout the growth plate; however, they still exhibited organized growth plate zones. Inhibition of cholesterol synthesis also resulted in rounded cellular morphology, except the chondrocytes looked much smaller and no hypertrophic zone was observed. Cytochalasin D treatment was unable to rescue the effects of lovastatin and HPCD treatment. However, addition of cholesterol was able to rescue the phenotype, and growth plate zones were clearly distinguishable. Data shown are representative, scale bar = 0.1 mm.

We confirmed that *Rora* mRNA expression was up-regulated in response to cytochalasin D treatment but not affected by the levels of cholesterol. We show here that *Fabp4, Cd36*, *Lpl* and *Klf15* mRNA levels are all responsive to cholesterol signalling and their up-regulation in the microarray are likely due to the increase in Ror-α expression and activity (Fig. 10). The regulation of genes implicated in lipid metabolism in chondrocytes is not without precedence, as previous work done by our lab has shown that chondrocytes are capable of lipid metabolism [36].

We also show that treatment of tibiae with cholesterol resulted in similar effects on bone growth as cytochalasin D, while inhibition of cholesterol synthesis resulted in much shorter bones and blocked the anabolic effects of cytochalasin D. Interestingly, because cytochalasin D cannot rescue the effects of HPCD/lovastatin treatment (in contrast to cholesterol), cytochalasin D appears to act upstream of and to require cholesterol signalling for its anabolic function. It is important to note that some of the effects of inhibiting cholesterol synthesis may be due to the inhibition of production of other mevalonate pathway members, such as farnesyl and geranylgeranyl side chains. Data from our lab has shown that members of the Rho family of proteins are important for chondrocyte maturation [24, 62]. Prenylation (farnesylation and/or geranylgeranylation) of this family of proteins is required for function and therefore cannot be ruled out as a contributing factor to the phenotypes observed [63]. However, because exogenous cholesterol can overcome the effects of these

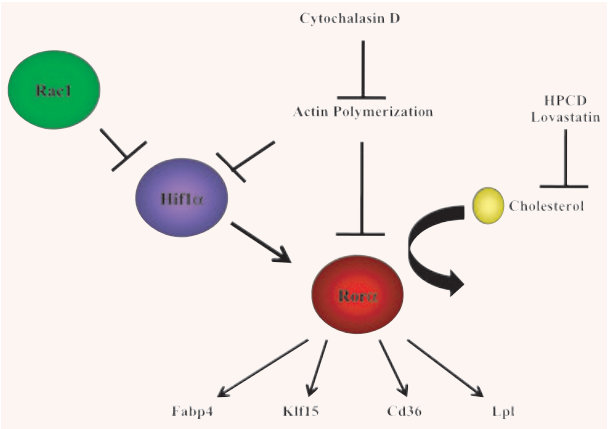

Fig. 10 Summary. Our studies suggest that a gene expressed during chondrocyte differentiation to hypertrophy, Ror-α, regulates the expression of Fabp4, Klf15, Cd36 and Lpl in a cholesterol dependent manner. Inhibition of actin polymerization by cytochalasin D or inhibition of Rac1 signalling promotes Ror-α expression levels. The regulation of Ror-α expression levels is likely mediated *via* Hif-1α, a known regulator of Ror-α.

inhibitors, it appears likely that altered cholesterol levels are responsible for the majority of the observed effects.

It is interesting to note that the well-characterized staggerer mouse which carries a loss-of-function mutation in the *Rora* gene displays dwarfism [64], but to our knowledge growth plate function has not been studied in these mice. Previous work has shown that inhibiting cholesterol synthesis decreases longitudinal growth and chondrocyte hypertrophy *in vivo* [65]. However, these findings were contributed to the decrease in necessary post-translational modification of sonic hedgehog and Indian hedgehog for activity. From our studies, we show that cholesterol itself may also be regulating chondrocyte hypertrophy directly, through activation of Ror-α and downstream target genes (*e.g.* genes involved in lipid metabolism).

Importantly, we show that Ror-α is not only induced by the relatively unphysiological compound cytochalasin D, but also up-regulated during physiological chondrocyte maturation *in vitro* and *in vivo*. Furthermore, we show that cartilage-specific inactivation of the Rac1 gene, a prominent regulator of actin dynamics, also results in increased expression of Ror-α and its upstream regulator Hif-1α. These data suggest novel links between regulators of cytoskeletal dynamics (*e.g.* Rac1 and possibly other Rho GTPases), oxidative signalling (*e.g.* Hif1a) and lipid metabolism (*e.g.* Rora) in the control of endochondral bone growth.

In summary, our data suggest that changes in actin dynamics in chondrocytes result in up-regulation of Ror-α expression, potentially through increased Hif-1α expression. Elevated levels of Ror-α mediate the anabolic response of endochondral bones to cholesterol. These data identify Ror-α as a novel regulator of endochondral bone growth at the intersection of actin dynamics, oxidative signalling and lipid metabolism.

Acknowledgements

A.W. and C.G.J. were supported by Doctoral Awards from the Canadian Institutes of Health Research (CIHR). F.B. is the recipient of a Canada Research Chair. This work was supported by operating grants from the CIHR and the Canadian Arthritis Network to F.B.

Supporting Information

Additional Supporting Information may be found in the online version of this article.

Table S1 Probe sets regulated by Y27632

Table S2 Probe sets regulated by cytochalasin D

Table S3 Probe sets regulated by jasplakinolide

Fig. S1 Gene ontology and Kegg pathways in response to Y27632 treatment
(**A**) Microarray gene sets from primary chondrocytes treated with 10 μM Y27632 for a period of 24 hrs were assessed according to GO annotations categorized by Fatigo+.
(**B**) Kegg annotations were used to determine common gene changes within different signalling pathways.

Fig. S2 Gene ontology and Kegg pathways in response to jasplakinolide treatment. (**A**) Microarray gene sets from primary chondrocytes treated with 50 nM jasplakinolide for a period of 24 hrs were assessed according to GO annotations categorized by Fatigo+.
(**B**) Kegg annotations were used to determine common gene changes within different signalling pathways.

This material is available as part of the online article from: http://www.blackwell-synergy.com/doi/abs/10.1111/j.1582-4934.2009.00684.x
(This link will take you to the article abstract).

Please note: Wiley-Blackwell are not responsible for the content or functionality of any supporting materials supplied by the authors. Any queries (other than missing material) should be directed to the corresponding author for the article.

References

1. **Hunziker EB.** Mechanism of longitudinal bone growth and its regulation by growth plate chondrocytes. *Microsc Res Tech*. 1994; 28: 505–19.
2. **Noonan KJ, Hunziker EB, Nessler J, *et al*.** Changes in cell, matrix compartment, and fibrillar collagen volumes between growth-plate zones. *J Orthop Res*. 1998; 16: 500–8.
3. **Abad V, Meyers JL, Weise M, *et al*.** The role of the resting zone in growth plate chondrogenesis. *Endocrinology*. 2002; 143: 1851–7.
4. **Hunziker EB, Schenk RK, Cruz-Orive LM.** Quantitation of chondrocyte performance in growth-plate cartilage during longitudinal bone growth. *J Bone Joint Surg Am*. 1987; 69: 162–73.
5. **Wilsman NJ, Farnum CE, Leiferman EM, *et al*.** Differential growth by growth plates as a function of multiple parameters of chondrocytic kinetics. *J Orthop Res*. 1996; 14: 927–36.
6. **Beier F.** Cell-cycle control and the cartilage growth plate. *J Cell Physiol*. 2005; 202: 1–8.
7. **Breur GJ, VanEnkevort BA, Farnum CE, *et al*.** Linear relationship between the volume of hypertrophic chondrocytes and the rate of longitudinal bone growth in growth plates. *J Orthop Res*. 1991; 9: 348–59.
8. **Karsenty G, Wagner EF.** Reaching a genetic and molecular understanding of skeletal development. *Dev Cell*. 2002; 2: 389–406.
9. **Schwartz NB, Domowicz M.** Chondrodysplasias due to proteoglycan defects. *Glycobiology*. 2002; 12: 57–68.
10. **Spranger J, Winterpacht A, Zabel B.** The type II collagenopathies: a spectrum of chondrodysplasias. *Eur J Pediatr*. 1994; 153: 56–65.
11. **Drissi H, Zuscik M, Rosier R, *et al*.** Transcriptional regulation of chondrocyte maturation: potential involvement of transcription factors in OA pathogenesis. *Mol Aspects Med*. 2005; 26: 169–79.
12. **Aigner T, Gerwin N.** Growth plate cartilage as developmental model in osteoarthritis reserach–potentials and limitations. *Curr Drug Targets*. 2007; 8: 377–85.
13. **James CG, Appleton CT, Ulici V, *et al*.** Microarray analyses of gene expression during chondrocyte differentiation identifies novel regulators of hypertrophy. *Mol Biol Cell*. 2005; 16: 5316–33.
14. **Woods A, Wang G, Beier F.** RhoA/ROCK signaling regulates Sox9 expression and actin organization during chondrogenesis. *J Biol Chem*. 2005; 280: 11626–34.
15. **Woods A, Beier F.** RhoA/ROCK signaling regulates chondrogenesis in a context-dependent manner. *J Biol Chem*. 2006; 281: 13134–40.
16. **Wang G, Woods A, Sabari S, *et al*.** RhoA/ROCK signaling suppresses hypertrophic chondrocyte differentiation. *J Biol Chem*. 2004; 279: 13205–14.
17. **Benya PD, Brown PD, Padilla SR.** Microfilament modification by dihydrocytochalasin B causes retinoid acid-modulated chondrocytes to re-express the differentiated collagen phenotype without a change in shape. *J Cell Biol*. 1988; 106: 161–70.
18. **Brown PD, Benya PD.** Alterations in chondrocyte cytoskeletal architecture during phenotypic modulation by retinoic acid and dihydrocytochalasin B-induced reexpression. *J Cell Biol*. 1988; 106: 171–9.
19. **Benya PD.** Modulation and re-expression of the chondrocyte phenotype; mediation by cell shape and microfilament modification. *Pathol Immunopathol Res*. 1988; 7: 51–4.
20. **Newman SA, Watt FM.** Influence of cytochalasin D induced changes in cell shape on proteoglycan sythesis by cultured articular chondrocytes. *Exp Cell Res*. 1988; 178: 199–210.
21. **Loty S, Forest N, Boulekbache H, *et al*.** Cytochalasin D induces changes in cell shape and promotes in vitro chondrogenesis: a morphological study. *Biol Cell*. 1995; 83: 149–61.
22. **Agoston H, Khan S, James CG, *et al*.** C-type natriuretic peptide regulates endochondral bone growth through p38 MAP kinase-dependent and independent pathways. *BMC Devl Biol*. 2007; 7: 18.
23. **Ulici V, Hoenselaar KD, Gillespie JR, *et al*.** The PI3K pathway regulates endochondral bone growth through control of hypertrophic chondrocyte differentiation. *BMC Dev Biol*. 2008; 11: 40.
24. **Wang G, Woods A, Agoston H, *et al*.** Genetic ablation of Rac1 in cartilage results in chondrodysplasia. *Dev Biol*. 2007; 306: 612–23.
25. **James CG, Ulici V, Tuckermann J, *et al*.** Expression profiling of dexamethasone treated primary chondrocyte identifies targets of glucocorticoid signaling in endochondral ossification development. *BMC Genomics*. 2007; 8: 205.
26. **Kang HS, Angers M, Beak JY, *et al*.** Gene expression profiling reveals a regulatory role for ROR alpha and ROR gamma in phase I and phase II metabolism. *Physiol Genomics*. 2007; 31: 281–94.
27. **James CG, Woods A, Underhill TM, *et al*.** The transcription factor ATF3 is upregulated during chondrocyte differentiation and represses cyclin D1 and A gene transcription. *BMC Mol Biol*. 2006; 7: 30.
28. **Bursell L, Woods A, James CG, *et al*.** Src kinase inhibition promotes the chondrocyte phenotype. *Arthritis Res Ther*. 2007; 9: R105.
29. **Bubb M, Senderowicz A, Sausville E, *et al*.** Jasplakinolide, a cytotoxic natural product, induces actin polyerization and competitively inhibits the binding of phalloidin to F-actin. *J Biol Chem*. 1994; 269: 14869–71.
30. **Goddette DW, Frieden C.** The kinetics of cytochalasin D binding to monomeric actin. *J Biol Chem*. 1986; 261: 15970–3.
31. **Miralles F, Posern G, Zaromytidou A-I, *et al*.** Actin dynamics control SRF activity by regulation of its coactivator MAL. *Cell*. 2003; 113: 329–42.
32. **Al-Shahrour F, Carbonell J, Minquez P, *et al*.** Babelomics: advanced functional profiling of transcriptomics, proteomics and genomics experiments. *Nucleic Acids Res*. 2008; 36: W341–6.
33. **Shao YY, Wang L, Hicks DG, *et al*.** Expression and activation of peroxisome proliferator-activated receptors in growth plate chondrocytes. *J Orthop Res*. 2005; 23: 1139–45.
34. **Hill TP, Spater D, Taketo MM, *et al*.** Canonical Wnt/beta-catenin signaling prevents osteoblasts from differentiating into chondrocytes. *Dev Cell*. 2005; 8: 727–38.
35. **Li TF, O'Keefe RJ, Chen D.** TGF-beta signaling in chondrocytes. *Front Biosci*. 2005; 1: 681–8.
36. **Stanton LA, Beier F.** PPARgamma2 expression in growth plate chondrocytes is regulated by p38 and GSK-3. *J Cell Mol Med*. DOI: 10.1111/j.1582-4934.2008.00396.x
37. **Enomoto-Iwamoto M, Kitagawa J, Koyama E, *et al*.** The Wnt antagonist Frzb-1 regulates chondrocyte maturation and long bone development during limb skeletogenesis. *Dev Biol*. 2002; 251: 142–56.

38. **Coleman CM, Tuan RS.** Functional role of growth/differentiation factor 5 in chondrogenesis of limb mesenchymal cells. *Mech Dev*. 2003; 120: 823–36.
39. **Cunningham NS, Jenkins NA, Gilbert DJ, *et al*.** Growth/differentiation factor-10: a new member of the transforming growth factor-beta superfamily related to bone morphogenetic protein-3. *Growth Factors*. 1995; 12: 99–109.
40. **Schipani E, Ryan HE, Didrickson S, *et al*.** Hypoxia in cartilage: HIF-1alpha is essential for chondrocyte growth arrest and survival. *Genes Dev*. 2001; 15: 2865–76.
41. **Chauvet C, Bois-Joyeux B, Berra E, *et al*.** The gene encoding human retinoic acid-receptor-related orphan receptor alpha is a target for hypoxia-inducible factor 1. *Biochem J*. 2004; 384: 79–85.
42. **Kallen JA, Schlaeppi JM, Bitsch F, *et al*.** X-ray structure of the hRORalpha LBD at 1.63 A: structural and functional data that cholesterol or a cholesterol derivative is the natural ligand of RORalpha. *Structure*. 2002; 10: 1697–707.
43. **Wiesenberg I, Missbach M, Kahlen JP, *et al*.** Transcriptional activation of the nuclear receptor RZR alpha by the pineal gland hormone melatonin and identification of CGP 52608 as a synthetic ligand. *Nucleic Acids Res*. 1995; 23: 327–33.
44. **Alberts AW, Chen J, Kuron G, *et al*.** Mevinolin: A highly potent competitve inhibitor of hydroxymethylglutaryl coenzyme A reductase and a cholesterol-lowering agent. *Proc Natl Acad Sci USA*. 1980; 77: 3957–61.
45. **Lau P, Nixon SJ, Parton RG, *et al*.** RORalpha regulates the expression of genes involved in lipid homeostasis in skeletal muscle cells: caveolin-3 and CPT-1 are direct targets of ROR. *J Biol Chem*. 2004; 279: 36828–40.
46. **Pfander D, Cramer T, Deuerling D, *et al*.** Expression of thrombospondin-1 and its receptor CD36 in human osteoarthritic cartilage. *Ann Rheum Dis*. 2000; 59: 448–54.
47. **Mic FA, Molotkiv A, Fan X, *et al*.** RALDH3, a retinaldehyde dehydrogenase that generates retinoic acid, is expressed in the ventral retina, otic vesical and olfactory pit during mouse development. *Mech Dev*. 2000; 97: 227–30.
48. **Gray S, Wang B, Orihuela Y, *et al*.** Regulation of gluconeogenesis by Kruppel-like factor 15. *Cell Metab*. 2007; 5: 305–12.
49. **Schnabel M, Marlovits S, Eckhoff G, *et al*.** Dedifferentiation-associated changes in morphology and gene expression in primary human articular chondrocytes in cell culture. *Osteoarthritis Cartilage*. 2002; 10: 62–70.
50. **Mallein-Gerin F, Garrone R, van der Rest M.** Proteoglycan and collagen synthesis are correlated with actin organization in dedifferentiating chondrocytes. *Eur J Cell Biol*. 1991; 56: 364–73.
51. **Woods A, Wang G, Beier F.** Regulation of chondrocyte differentiation by the actin cytoskeleton and adhesive interactions. *J Cell Physiol*. 2007; 213: 1–8.
52. **Uribe R, Jay D.** A review of actin binding proteins: new perspectives. *Mol Biol Rep*. 2009; 36: 121–5.
53. **Loy CJ, Sim KS, Yong EL.** Filamin-A fragment localizes to the nucleus to regulate androgen receptor and coactivator functions. *Proc Natl Acad Sci USA*. 2003; 100: 4562–7.
54. **Gerber HP, Vu TH, Ryan AM, *et al*.** VEGF couples hypertrophic cartilage remodeling, ossification and angiogenesis during endochondral bone formation. *Nat Med*. 1999; 5: 623–8.
55. **Shen Z, Gantcheva S, Mansson B, *et al*.** Chondradherin expression changes in skeletal development. *Biochem J*. 1998; 330: 549–57.
56. **Dreier R, Opolka A, Grifka J, *et al*.** Collagen IX-deficiency seriously compromises growth cartilage development in mice. *Matrix Biol*. 2008; 27: 319–29.
57. **Hasky-Negev M, Simsa S, Tong A, *et al*.** Expression of matrix metalloproteinases during vascularization and ossification of normal and impaired avian growth plate. *J Anim Sci*. 2008; 86: 1306–15.
58. **Steinmayr M, Andre E, Conquet F, *et al*.** Staggerer phenotype in retinoid-related orphan receptor alpha-deficient mice. *Proc Natl Acad Sci USA*. 1998; 95: 3960–5.
59. **Raspe E, Duez H, Gervois P, *et al*.** Transcriptional regulation of apolipoprotein C-III gene expression by the orphan nuclear receptor RORalpha. *J Biol Chem*. 2001; 276: 2865–71.
60. **Meyer T, Kneissel M, Mariani J, *et al*.** In vitro and in vivo evidence for orphan nuclear receptor RORalpha function in bone metabolism. *Proc Natl Acad Sci USA*. 2000; 97: 9197–202.
61. **Kopmels B, Mariani J, Delhaye-Bouchaud N, *et al*.** Evidence for a hyperexcitability state of staggerer mutant mice macrophages. *J Neurochem*. 1992; 58: 192–9.
62. **Wang G, Beier F.** Rac1/Cdc42 and RhoA GTPases antagonistically regulate chondrocyte proliferation, hypertrophy, and apoptosis. *J Bone Miner Res*. 2005; 20: 1022–31.
63. **Seabra MC.** Membrane association and targeting of prenylated Ras-like GTPases. *Cell Signal*. 1998; 10: 167–72.
64. **Sidman RL, Lane PW, Dickie MM.** Staggerer, a new mutation in the mouse affecting the cerebellum. *Science*. 1962; 137: 610–2.
65. **Wu S, De Luca F.** Role of cholesterol in the regulation of growth plate chondrogenesis and longitudinal bone growth. *J Biol Chem*. 2004; 279: 4642–7.